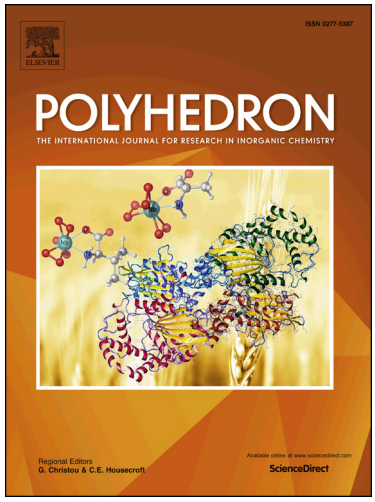

Synthesis and Characterization of Cu(II) Complexes of 2-amino-6–sulfamoyl-benzothiazole and Their Inhibition Studies on Carbonic Anhydrase Isoenzymes

Zeynep Alkan Alkaya, Halil İlkimen, Cengiz Yenikaya, Ekrem Tunca, Metin Bülbül, Tuncay Tunç, Musa Sarı

PII: S0277-5387(18)30253-5
DOI: https://doi.org/10.1016/j.poly.2018.05.015
Reference: POLY 13162

To appear in: *Polyhedron*

Received Date: 6 April 2018
Accepted Date: 6 May 2018

Please cite this article as: Z.A. Alkaya, H. İlkimen, C. Yenikaya, E. Tunca, M. Bülbül, T. Tunç, M. Sarı, Synthesis and Characterization of Cu(II) Complexes of 2-amino-6–sulfamoylbenzothiazole and Their Inhibition Studies on Carbonic Anhydrase Isoenzymes, *Polyhedron* (2018), doi: https://doi.org/10.1016/j.poly.2018.05.015

Synthesis and Characterization of Cu(II) Complexes of 2-amino-6-sulfamoylbenzothiazole and Their Inhibition Studies on Carbonic Anhydrase Isoenzymes

Zeynep Alkan Alkaya[a], Halil İlkimen[b], Cengiz Yenikaya[b*], Ekrem Tunca[c], Metin Bülbül[c], Tuncay Tunç[d], Musa Sarı[e]

[a]*Department of Chemistry and Chemical Processing Technologies, Banaz Vocational School, Usak University, 64500 Banaz, Uşak, Turkey.*

[b]*Department of Chemistry, Faculty of Arts and Sciences, Dumlupınar University, 43100 Kütahya, Turkey.*

[c]*Department of Biochemistry, Faculty of Arts and Sciences, Dumlupınar University, 43100 Kütahya, Turkey.*

[d]*Department of Science Education, Faculty of Education, Aksaray University, 68100, Aksaray, Turkey.*

[e]*Department of Physics Education, Gazi University, 06500 Ankara, Turkey.*

*Corresponding Author: Cengiz Yenikaya

Department of Chemistry, Dumlupınar University, Kutahya Turkey

e-mail: cengiz.yenikaya@dumlupinar.edu.tr

Abstract:

2-Amino-6-sulfamoylbenzothiazole (SMABT) and its proton transfer compound $(HSMABT)^{+}(HDPC)^{-}$ (**1**) with 2,6-pyridinedicarboxylic acid (H_2DPC), and their Cu(II) complexes (**2** of SMABT, **3** and **4** of **1**) have been prepared and characterized by spectroscopic techniques. Additionally, single crystal X-ray diffraction techniques were applied to all complexes. All compounds, including acetazolamide (AAZ) as the control compound, were also evaluated for their *in vitro* inhibition effects on human hCA I and hCA II for their hydratase and esterase activities. The synthesized complexes have remarkable inhibitory effects on hCA I and hCA II isoenzymes. The inhibition potentials of the proton transfer salt (**1**) and the metal complexes (**2-4**) are comparable with AAZ. Esterase K_i values of the compounds (**1**-**4**) are in the range of 0.089±0.008 μM-0.149±0.017 μM for hCA I and 0.046±0.008 μM-0.085±0.019 μM for hCA II. Inhibition data have been analyzed by using a one-way analysis of variance for multiple comparisons ($p < 0.0001$).

***Keywords*:** 2-amino-6-sulfamoylbenzothiazole, proton transfer, metal complex, carbonic anhydrase, statistical analyses.

Introduction

The sulfamoyl and benzothiazole derivatives constitute an important class of drugs, with several types of pharmacological agents possessing, among others, antibacterial, anticonvulsant, anti-inflammatory, antitubercular, therapeutic, protease, and carbonic anhydrase inhibitory effects [1-3].

The metal complexes for 2,6-pyridinedicarboxylic acid (or dipicolinic acid, H_2DPC) and its deprotonated forms ($HDPC^-$ and DPC^{2-}) show interesting structural features with various coordination modes [4], stabilization of unusual oxidation states [5] and insulin-mimetic effects [6,7]. H_2DPC with Cu(II) ion commonly has one or two coordination modes [4]. In one coordination mode, a single planar DPC ligand associates in the equatorial plane of a metal cation with other ligands such as, H_2O or pyridine-based heterocycles [4,8], which occupy the remaining sites. This leads to the formation of square pyramidal [4,9-13] or octahedral coordination geometry [4,10-12,14]. In the second coordination mode, two perpendicularly coordinated planar dipicolinic molecules generate distorted octahedral coordination geometry [4,9,10,14].

In this study, 2-amino-6-sulfamoylbenzothiazole (SMABT) [15] and proton transfer compound $(SMHABT)^+(HDPC)^-$ (**1**) [17] have been prepared according to literature. Their Cu(II) complexes have been also prepared between SMABT and Cu(II) in order to give (**2**) as a simple complex, and between **1** and Cu(II) to give **3** which is an ionic complex containing $(SMHABT)^+$ and $[Cu(DPC)_2]^{2-}$ ions, and also **4** which is a nonionic mixed ligand complex as $\{[Cu(DPC)(SMABT)(H_2O)]_2H_2O\}$. The mixed ligand metal complexes have generally shown better biological activities which are better than those of the simple ones [8-14]. They are characterized by elemental, spectral (IR and Uv-Vis.) and thermal analyses, as by using magnetic measurement and molar conductivity techniques. Single crystal X-ray diffraction

techniques were applied to all complexes (**2-4**). The simple Cu(II) complex of H_2DPC [17] has also been prepared in order to compare the inhibition data of all studied compounds.

In addition, we have investigated the potential use of these compounds as new inhibitors of human carbonic anhydrase isoenzymes, hCA I and hCA II. Carbonic anhydrases (CAs, EC 4.2.1.1) are ubiquitous metalloenzymes used to catalyze interconversion of carbon dioxide and water to produce bicarbonate and proton, and are encoded by seven unrelated gene families: α-, β-, γ-, δ-, ζ-, η-, and θ-CAs [18]. There are sixteen α-CA isoforms or CA-related proteins identified in mammals [19]. Among the α-CAs, hCA I is major CA isoform, and hCA II is also present in the human eye [20]. hCA II participates in aqueous humor secretion [21], and the inhibition of this isoenzyme is extremely important in the treatment of glaucoma, which is a group of diseases characterized by the gradual loss of visual field due to an elevation in intraocular pressure (IOP) [21,22].

2. Experimental section

2.1. General methods and materials

All chemicals used were analytical reagents and were commercially purchased from Aldrich. Elemental analyses for C, H, N and S were performed on Elementar Vario III EL and Cu were detected with Perkin Elmer Optima 4300 DV ICP-OES. Crystallographic data were recorded on a Bruker Kappa APEX II CCD area-dedector X-ray diffractometer. FT-IR spectra were recorded in the 4000-400 cm^{-1} region with Bruker Optics, Vertex 70 FT-IR spectrometer using ATR techniques. Thermal analyses were performed on Pelkin Elmer SII Exstar 6000 TG/DTA 6300 model using platinum crucible with 10 mg sample. Measurements were taken in the static air within a 30-900 ºC temperature range. The UV–Vis spectra were obtained for DMSO solution of the compounds (10^{-3} M) with a SHIMADZU UV-2550 spectrometer in the range of 200–900 nm. Magnetic susceptibility measurements at room temperature were

performed using a Sherwood Scientific Magway MSB MK1 model magnetic balance by the Gouy method using $Hg[Co(SCN)_4]$ as calibrant. The molar conductances of the compounds were determined in water/ethanol (1:1) and in DMSO (10^{-3} M) at room temperature using a WTW Cond 315i/SET Model conductivity meter.

2.2. Synthesis of metal complexes (2-4)

2-Amino-6-sulfamoylbenzothiazole (SMABT) [15] and proton transfer compound $(SMHABT)^+(HDPC)^-$ (**1**) [16] have been prepared according to literature (Figures S1-S5 and Tables S1-S3)

A solution of 1 mmol (0.199 g) $Cu(CH_3COO)_2.H_2O$ in water (10 mL) was added dropwise to the solution of 1 mmol (0.229 g) SMABT for **2** or to the solution of 1 mmol of (0.396 g) **1** for **3** in water/ethanol (1:1) (20 mL) with stirring at room temperature for one day. The reaction mixture was kept at room temperature for two weeks to give green crystalline solid for **2** (0.331 g, 45% yield), green crystalline solid for **3** (0.106 g, %40 yield). Compound **4** was obtained from the mother liquor of **3** after one week as turquoise crystalline solid (0.109 g, 45% yield) (Fig.1). The single crystals of all complexes suitable for X-ray diffraction were separated and washed with EtOH/water (1:1).

Anal. Calcd. for **2** ($C_{23}H_{32}N_6O_{12}S_4Cu_4$): C, 32.89%; H, 3.84%; N, 10.01%; S, 15.27%; Cu, 15.12%. Found: C, 32.85%; H, 3.80%; N, 10.05%; S, 15.30%; Cu, 15.15%; for **3** ($C_{28}H_{32}N_8O_{17}S_2Cu$): C, 35.61%; H, 3.42%; N, 11.87%; S, 13.58%; Cu, 6.73%. Found: C, 35.65%; H, 3.40%; N, 11.85%; S, 13.60%; Cu, 6.75%.; for **4** ($C_{28}H_{26}N_8O_{15}S_4Cu_2$): C, 34.67%; H, 2.70%; N, 11.55%; S, 13.22%; Cu, 13.10%. Found: C, 34.70%; H, 2.70%; N, 11.60%; S, 13.60%; Cu, 13.15%.

The experimental studies of purification of carbonic anhydrase I and II isoenzymes from human erythrocytes, determination of hydratase and esterase activities of hCA I and

hCA II, determination of IC_{50} and K_i values of the compounds and statistical analysis are given in the Supplementary file [23-29].

2.3. X-ray data collection and structure refinement

The crystal and instrumental parameters used in the unit-cell determination and data collection are summarized in Table 1 for the compounds **2-4**. Crystallographic data of **2-4** were recorded on a Bruker Kappa APEX II CCD area-dedector X-ray diffractometer employing plane graphite monochromatized with MoK_α radiation (λ = 0.71073 Å), using ω-2θ scan mode. The empirical absorption corrections were applied by multi-scan via Bruker, SADABS software [30]. The structures were solved by the direct methods and subsequently completed by difference Fourier recycling. All non-hydrogen atoms were refined anisotropically using the full-matrix least-squares techniques on F^2. The SHELXS-97 and SHELXL-97 [31] programs were used for all the calculations. The H atoms were placed in idealized positions and constrained to ride on their parent atoms with distances in the range of N-H = 0.71(6)-0.92(9) Å, C-H = 0.93-0.96Å and with U_{iso}(H)= 1.2Ueq(C,N) or 1.5Ueq(C) for methyl atoms. The H atoms of water molecules were located from in a difference Fourier maps and were constrained at distance of O-H = 0.74(3)-0.83(4) Å and with U_{iso}(H) = 1.5Ueq(O). The drawings of molecules were accomplished with the help of ORTEP-3 for Windows [32].

3. Results and discussion

3.1. Crystal structures of 2-4

The molecular structures of **2-4**, with the atom labeling of symmetric units, are shown in Figures 2-4, respectively. The details of the crystal structure solutions are summarized in Table 1 and the selected bond lengths and angles are listed in Table 2.

Table 1. Crystal data and structure refinement details for compounds **2-4.**

	2	**3**	**4**
Empirical formula	$C_{22}H_{30}Cu_2N_6O_{14}S_4$	$C_{28}H_{32}CuN_8O_{17}S_4$	$C_{28}H_{26}Cu_2N_8O_{15}S_4$
Formula weight	857.86	944.41	969.91
T[K]	296(2)	296(2)	296(2)
Wavelength (Å)	0.71073	0.71073	0.71073
Crystal system, space group	Triclinic, $P\bar{1}$	Triclinic, $P\bar{1}$	Monoclinic, $P21/c$
Unit cell dimensions (Å, º)			
a	8.0679(4)	9.245(5)	14.7958(9)
b	8.2980(4)	14.425(5)	20.4121(14)
c	13.0375(6)	14.574(5)	11.9090(8)
α	104.927(2)	98.617(5)	
β	97.568(2)	106.710(5)	104.300(2)
γ	90.597(2)	90.774(5)	
V ($Å^3$)	835.13(7)	1837.2(13)	3485.2(4)
Z	1	2	4
Absorbtion coefficient (mm^{-1})	1.596	0.910	1.546
D_{calc} (Mg/m^3)	1.595	1.707	1.849
F(000)	438	970	1968
Crystal dimensions (mm)	0.25x0.14x0.10	0.25x0.16x0.10	014x0.10x0.08
θ range for data collection (º)	1.63-28.49	1.88-28.60	2.81-26.36
Index ranges	$-10\leq h\leq 10$	$-12\leq h\leq 12$	$-18\leq h\leq 18$
	$-11\leq k\leq 11$	$-19\leq k\leq 19$	$-25\leq k\leq 25$
	$-17\leq l\leq 17$	$-19\leq l\leq 19$	$-14\leq l\leq 14$
Reflections collected	15630	34222	77224
Independent reflections	4233	9401	9792
Data/parameters	3795/235	7708/595	7175/571
Max. and min. transmission	0.765, 0.852	0.840, 0.913	0.881, 0.884
Final R indices [$I\geq 2\sigma(I)$]	$R_2 = 0.0300$	$R_2 = 0.0336$	$R_2 = 0.0270$
	$wR_2 = 0.0745$	$wR_2 = 0.0935$	$wR_2 = 0.0637$
R indices (all data)	$R_1 = 0.0264$	$R_1 = 0.0431$	$R_1 = 0.0364$
	$wR_1 = 0.0720$	$wR_1 = 0.0880$	$wR_1 = 0.0687$
Goodness-of-fit on F^2	1.038	1.030	1.054
Largest difference in peak and hole ($e\ Å^{-3}$)	0.424, -0.403	0.368, -0.443	0.343, -0.393

Table 2. Selected bond distances [Å] and angles [°] of compounds **2-4.**

Compound **2**: $[Cu_2(SMABT)_2(Ac)_2].2H_2O$					
Cu1-O3	1.9613(14)	Cu1-O2	1.9779(14)	Cu1-N1	2.1899(14)
Cu1-O4	1.9708(14)	Cu1-O1	1.9852(14)	Cu1-Cu1^{i}	2.6515(4)
O1-Cu1-N1	98.89(6)	O3-Cu1-O1	90.39(6)	O4-Cu1-O1	88.79(7)
O1-Cu1-Cu1^{i}	85.00(4)	O3-Cu1-O2	88.84(7)	O4-Cu1-O2	89.28(7)
O2-Cu1-O1	167.53(6)	O3-Cu1-O4	167.49(6)	O4-Cu1-N1	95.30(6)
O2-Cu1-N1	93.55(6)	O3-Cu1-N1	97.16(6)	O4-Cu1-Cu1^{i}	84.62(4)
O2-Cu1-Cu1^{i}	82.56(4)	O3-Cu1-Cu1^{i}	82.87(4)	N1-Cu1-Cu1^{i}	176.11(4)
Compound **3**: $(HSMABT)_2[Cu(DPC)_2].5H_2O$					
Cu1-O1	2.2389(17)	Cu1-O5	2.2172(15)	Cu1-N1	1.9538(15)
Cu1-O2	2.1632(17)	Cu1-O6	2.1281(15)	Cu1-N2	1.9387(15)
N2 Cu1 N1	178.35(6)	O6 Cu1 O2	97.53(7)	N2 Cu1 O1	102.35(5)
N2 Cu1 O6	79.22(5)	N2 Cu1 O5	76.47(5)	N1 Cu1 O1	76.31(5)
N1 Cu1 O6	101.68(5)	N1 Cu1 O5	102.54(5)	O6 Cu1 O1	90.06(7)
N2 Cu1 O2	102.77(6)	O6 Cu1 O5	155.47(5)	O2 Cu1 O1	154.70(5)
N1 Cu1 O2	78.52(6)	O2 Cu1 O5	91.04(7)	O5 Cu1 O1	91.90(6)
Compound **4**: $[Cu(DPC)(SMABT)(H_2O)][Cu(DPC)(SMABT)(H_2O)].H_2O$					
Cu1-O1	2.0454(14)	Cu1-O1w	2.2263(18)	Cu2-N6	2.0069(17)
Cu1-O3	2.0286(15)	Cu2-O7	2.0230(16)	Cu2-O2w	2.321(2)
Cu1-N1	1.9317(17)	Cu2-O9	2.0645(16)		
Cu1-N2	1.9980(17)	Cu2-N5	1.9312(18)		
N1 Cu1 N2	170.64(7)	N1 Cu1 O1w	97.34(7)	N5 Cu2 O9	79.00(7)
N1 Cu1 O1	78.71(6)	N2 Cu1 O1w	91.69(7)	N6 Cu2 O9	105.28(7)
N1 Cu1 O3	79.33(6)	O3 Cu1 O1w	95.51(7)	O7 Cu2 O9	157.72(7)
N2 Cu1 O3	97.40(6)	N5 Cu2 N6	173.19(7)	N5 Cu2 O2w	91.27(7)
N2 Cu1 O1	102.70(6)	N5 Cu2 O7	79.09(7)	N6 Cu2 O2w	93.95(7)
O3 Cu1 O1	155.88(6)	N6 Cu2 O7	96.17(7)	O7 Cu2 O2w	93.82(8)

Symmetry code: (i) *–x+1, –y+1, –z+1*

The complex **2** crystallizes in the triclinic $P\bar{1}$ space group. The structure of **2** has a crystallographic inversion centre. The symmetric unit of **2**, $[Cu_2(SMABT)_2(CH_3COO)_4].2H_2O$, contains two SMABT molecules, four acetate anions as bridges, two Cu(II) cations and two uncoordinated water molecules. The coordination

environment of the two Cu(II) ions (Cu1 and Cu1^{i}) can be described as distorted octahedron with each Cu(II) atom being surrounded by four μ^2-bridging bidentate acetate ligands in the basal plane and one SMABT molecule in one axial position. In the structure, each acetate molecules form distorted rectangle planes [Cu1-O3, O3-O4, O4-Cu1^{i}, Cu1-Cu1^{i}] around each metal ion (the bond lengths for Cu-O between 1.9613(14) and 1.9852(14) Å), while the Cu(II) ions are displaced by 0.428(4) Å from these planes towards the N atoms (Cu-N 2.1899(14) Å). The N1-Cu1-Cu1^{i} *trans*-angle is much closer to 180° (176.11(4)°). Finally, the sixth coordination comes from Cu1-Cu1^{i} metallic bond (2.6515(4) Å) (Table 2).

The complex **3** crystallizes in the triclinic $P\bar{1}$ space group. The structures of **3**, $(SMHABT)_2[Cu(DPC)_2].5H_2O$, consist of one $[Cu(DPC)_2]^{2-}$ anion and two counter $SMHABT^+$ cations, and five uncoordinated water molecules. In complex **3**, the Cu(II) ion is coordinated by four oxygen atoms (O1, O2, O5 and O6) and two nitrogen atoms (N1 and N2) of two DPC^{2-} ions resulting with a distorted octahedral conformation. Both carboxylate oxygen atoms from DPC^{2-} occupy the *trans*-apical positions of the Cu(II) coordination polyhedron with bond lengths [Cu1-O1 = 2.2389(17) Å, Cu1-O5 = 2.2172(15) Å, Cu1-O2 = 2.1632(17) Å and Cu1-O6 = 2.1281(15) Å], and define low *trans*-angle value around Cu(II) ion as 154.70(5)° for O2-Cu1-O1 and 155.47(5)° for O6-Cu1-O5 which reveals a rather rigid structure of such tri-dentate ligands. In contrast, the N1-Cu1-N2 *trans*-angle is much closer to 180° (178.35(6)°) and the dihedral angle defined by the mean planes of two DPC ligands is 102.35(5)° showing that they fall almost perpendicular.

The complex **4** crystallizes in the monoclinic P21/c space group. The symmetric unit of **4**, $[Cu(DPC)(SMABT)(H_2O)][Cu(DPC)(SMABT)(H_2O)].H_2O$, consists of two independent and similar molecules, each containing one coordinated DPC^{2-} ion, one coordinated SMABT molecule, one coordinated water molecule and one Cu(II) ion, and additionally one uncoordinated water molecule for both independent centers (Figure 4). Each Cu^{2+} ions is

coordinated by two N atoms, one from DPC (N1 for Cu1 and N5 for Cu2) and one from SMABT ring (N2 for Cu1 and N6 for Cu2), by two carboxylate O atoms from DPC (O1 and O3 for Cu1 and O7 and O9 for Cu2) and with the axial site occupied by the one coordinated water molecule (O1w for Cu1 and O2w for Cu2) (Fig. 4). Thus the coordination environment of Cu^{2+} ions (for both molecule) have distorted square pyramid geometries with the structural index τ, 0.25 for Cu1 and 0.26 for Cu2 [33]. Two N atoms from two different ligands, DPC and SMABT, occupy equatorial positions (Fig. 4 and Table 2). The Cu-O_{water} bond distances, arising from coordination of the water molecule to the central metal ion, are 2.2263(18) Å for Cu1-O1w and 2.321(2) Å for Cu2-O2w, which are much longer than the Cu-O (carboxylate) bond distances (Table 2).

In all essential details, the geometries of the complexes (**2-4**) regarding bond lengths and angles are in good agreement with the values observed in similar Cu(II) complexes [8-11,13,34,35]. Cu-Cu metal bond length for **2** is also comparable with a very similar structure [34-36].

Hydrogen bonds for the complexes play important roles in stabilizing the crystal structures. The ranges of the D-H…A angles and those of the H…A and D…A distances indicate the presence of strong and weak hydrogen bondings in the structures **3** and **4** (Table 3).

Table 3. Hydrogen bonds for compounds **3** and **4** (Å, °)

D-H…A	d(D-H)	d(H…A)	d(D…A)	<D-H…A
3				
N3-H3B-O4w	0.79(3)	2.19(3)	2.894(3)	149(2)
N4-H4-O1	0.86	1.84	2.643(2)	154.6
N7-H7-O5	0.86	1.88	2.616(2)	143.2
O2w-H2C-O2	0.840(10)	2.03(2)	2.849(3)	163(6)
O3w-H3C-O2w	0.823(10)	1.992(12)	2.802(3)	168(3)
4				
N3-H31-O3	0.82(3)	1.95(3)	2.683(3)	149(3)
N7-H7B-O7	0.86(3)	1.86(3)	2.652(3)	151(3)

3.2. FT-IR measurements

The infrared spectral data of the starting compounds (SMABT, H_2DPC and **1**) and compounds **2**-**4** are given in Table S3. In the high frequency region, weak bands 3098-3067 cm^{-1} are attributed to the stretching vibrations of aromatic C-H for all compounds. There are also broad absorption bands at 3504-3424 cm^{-1}, which are attributed to the ν(OH) vibrations of water molecules for compounds **2-4**. The relatively weak and broad bands at 2752 and 2522 cm^{-1} are attributed to the ν(N^+-H) vibration for **3** [37]. The absorption bands at 3423, 3324, 3293 and 3237 cm^{-1} of NH_2 group of SMABT are slightly shifted from those found for **1** (3433, 3424, 3385 and 3229 cm^{-1}), for **2** (3422, 3358, 3229 and 3228 cm^{-1}), for **3** (3408, 3385, 3325 and 3244 cm^{-1}) and for **4** (3358, 3327, 3292 and 3237 cm^{-1}) due to the weak intermolecular interactions. The carboxylate groups for compounds H_2DPC and **1-4** exhibit strong carbonyl bands in the region of 1705–1456 cm^{-1}. These bands are reflected by IR spectrum of the asymmetric (ν_{as}) and symmetric (ν_s) stretching vibrations at 1701 and 1456 cm^{-1} for H_2DPC, 1705 and 1465 cm^{-1} for **1**, 1647 and 1422 cm^{-1} for **3**, 1648 and 1452 cm^{-1} for **4** from DPC^{2-} ions, 1590 and 1450 cm^{-1} for **2** from Ac^- ion. The differences (Δυ) between the asymmetric and symmetric stretches of the carboxylate groups of **2-4** are 140, 195, and 196, respectively, which suggest bridging for **2** and monodentate for **3** and **4**, binding of the carboxylate group to the metal ion [38]. The strong absorption bands in the region of 1637-1445 cm^{-1} are attributed to the *ν*(C=N) and *ν*(C=C) vibrations for all compounds. The vibrations of the *ν*(S=O) are also observed in the 1432-1098 cm^{-1} region for compounds SMABT and **1-4**. The C–O vibrations data for all compounds except SMABT are between 1363 and 1069 cm^{-1} as expected. The ring wagging vibrations of the pyridine groups are also observed in the 801-702 cm^{-1} region for compounds H_2DPC and **1**, **3** and **4**. The weak bands

at 459-436 cm^{-1} and 585-574 cm^{-1} are from the M–N and M–O vibrations of the compounds **2-4**.

3.3. Thermal analyses of all complexes

Figures S6-S8 show the TG-DTG and DTA curves of the compounds **2-4**, and the thermal analyses results are given in Table S4.

For the compound **2**, the first endothermic peak corresponds to the loss of two moles of water. The endothermic second stage is consistent to the loss of the four moles of acetate ions. The third stage, an exothermic peak, agrees to the loss of the $C_{12}H_{10}N_2O_4S_2$ unit and the $C_2H_4N_4S_2$ unit is decomposed exothermically in the following stage. The final decomposition product is CuO identified by IR spectroscopy.

For the compounds **3** and **4**, the first stage, an endothermic peak corresponds to the loss of water molecules, namely five moles for **3** and three moles for **4**. The exothermic second stage is consistent with the loss of the following units $C_{12}H_{10}N_2O_4S_4$ for **3** and $C_{10}H_{10}N_2O_4S_2$ for **4**. The units are also decomposed exothermically in the third stage: $C_{16}H_{12}N_6O_8$ for **3** and $C_{18}H_{16}N_6O_9S_2$ for **4**. The final decomposition products are CuO for **3** and **4**, and they are identified by IR spectroscopy.

3.4. UV/vis Spectrum, magnetic susceptibility and molar conductivity

The electronic spectra of compounds **1-4** and the free ligands SMABT and H_2DPC were recorded in DMSO solution with $1x10^{-3}$ $molL^{-1}$ concentrations at room temperature (Table S5, Figure S9). The characteristic π- π* transitions in the spectrum of **1** are of 305 nm and 290 nm, 288 nm and 271 nm for **2**, 304 nm and 290 nm for **3**, and 307 nm and 298 nm for **4**, with the same profiles as the free ligands SMABT (305 nm and 290 nm) and H_2DPC (303

nm). The bands for the d-d transitions in DMSO are observed at 760 nm for **2**, 752 nm for **3**, and 748 for **5**.

The room temperature magnetic moment of the metal complexes is of 1.70 BM for **2**, 1.67 BM for **3**, and 1.64 BM for **4** per metal ion, indicating the presence of one unpaired electron (Cu^{2+}, d^9) for all compounds.

The molar conductivity data in DMSO are of 4.5 $\Omega^{-1}cm^2mol^{-1}$ for **2**, 51.2 $\Omega^{-1}cm^2$ mol^{-1} for **3**, and 3.6 $\Omega^{-1}cm^2$ mol^{-1} for **4**, indicating that the complexes **2** and **4** are non-ionic, and the complex **3** is ionic with a 2:1 ratio [39].

3.5. In vitro inhibition studies

In this study the inhibition effects of proton transfer salt (**1**) and its metal complexes (**3** and **4**), and metal complex of SMABT (**2**) on the hydratase and esterase activities of human cytosolic carbonic anhydrases, hCA I and hCA II, have been investigated as in vitro. Inhibition potentials of these compounds were compared with starting compounds (SA, TBS, SMABT and H_2DPC) and reference compound, AAZ. No inhibitory effect of H_2DPC on the enzyme was observed. In contrast, other starting compounds, proton transfer salt and metal complexes inhibited both hydratase and esterase activities of isozymes. It is clearly observed that the synthesized compounds are more selective towards clinically important isoform, hCA II (Table 4).

When the inhibition of hydratase activity is examined, it is observed that the proton transfer salt and metal complexes are more potent inhibitors than starting compounds. This is especially pronounced for **2**-**4** compounds, and even the inhibition potencies of compounds **3** and **4** are comparable to AAZ. The proton transfer salt (**1**) formed between H_2DPC and SMABT increased the inhibition effect of SMABT and the coordination structure of this compound with Cu (II) maximizes its inhibition effect. In metal complexes, the number of

SMABT ligands is more than one and they can interact more strongly with the active site of the enzyme resulting excess inhibition effect of the metal complexes. It is remarkable that the inhibitory effect on the hydratase activity of compounds **3** and **4** is about 25-fold higher than that of the SMABT.

Table 4. The inhibition data and K_i values of hCA I and hCA II isozymes for hydratase and esterase activity.

Bileşik	Hidrataz IC_{50} (µM)[a,b]		Esteraz IC_{50} (µM) [a,b]		K_i (µM) [a,b]	
	hCA I	hCA II	hCA I	hCA II	hCA I	hCA II
AAZ[c]	0.390±0.008	0.200±0.005	0.420±0.004	0.310±0.008	0.260±0.003	0.140±0.005
SA	30.44±0.008	5.67±0.003	28.14±0.012	5.36±0.005	26.32±0.009	4.14±0.011
TBS	7.846±0.005	4.334±0.021	0.499±0.010	0.234±0.006	0.268±0.007	0.114±0.003
H_2DPC	No Inhibition	No Inhibition	No Inhibition	No Inhibition	No Inhibition	No Inhibition
CuDPC	No Inhibition	No Inhibition	No Inhibition	No Inhibition	No Inhibition	No Inhibition
SMABT	6.348±0.012	3.876±0.014	0.567±0.008	0.322±0.006	0.306±0.004	0.162±0.010
1	4.075±0.018	1.998±0.009	0.258±0.017	0.133±0.015	0.149±0.017	0.085±0.019
2	1.724±0.006	0.716±0.006	0.201±0.022	0.121±0.012	0.098±0.015	0.046±0.008
3	0.245±0.012	0.132±0.008	0.245±0.003	0.112±0.009	0.099±0.006	0.053±0.008
4	0.267±0.009	0.140±0.004	0.267±0.009	0.125±0.012	0.089±0.008	0.048±0.009

[a]Mean ± standard error, from three different assays.
[b]$p < 0.0001$ for all analysis.
[c]AAZ was used as reference compound.

While the inhibition profile of the esterase activity of the compounds resembles the inhibition of hydratase activity, sharp inhibition differences among the studies compounds for the inhibition of hydratase activity are not found for the inhibition of esterase activity. However, the synthesized compounds (**1**-**4**) exhibit about 2-3 times more potent inhibitory properties than the SMABT compound. This increase in the inhibition of esterase activity among the studied compounds can be attributed to the formation of the proton transfer salt and the formation of coordination with Cu(II) which is analogous to the inhibition of hydratase activity. In addition, another remarkable phenomenon in the inhibition of esterase activity is that the differences between the inhibition potencies of the compounds **1**-**4** are not

so great. The most prominent feature of our study of inhibition of esterase activity is that compounds **1**-**4** are more potent inhibitors than the AAZ compound.

The inhibition equilibrium constants (K_i values) of the compounds have been determined by using esterase activity measurements. The K_i constants of the compounds **1**-**4** indicate that these compounds have stronger inhibitory effects than the AAZ compound (Table 4). These results are important for designing potent inhibitors of hCA I and hCA II, which are cytosolic isoforms. The inhibitor compounds synthesized within the scope of the study can be modified to develop both more potent and more selective compounds against the hCA II isoenzyme.

4. Conclusion

In the present work, three newly Cu(II) complexes (**2-4**) were prepared for the first time. The complexes **2** and **3** crystallize in the triclinic $P\overline{1}$ space group, whereas the complex **4** crystallizes in the monoclinic P21/c space group. In the complex **2**, two Cu(II) ions are connected to each other with a Cu-Cu bond and with four bridged acetate ions. Each Cu(II) ions has also Cu-N bond from SMABT to give distorted octahedral geometry around Cu(II) ions. In complex **3**, the Cu(II) ion coordinates to four oxygen atoms and two nitrogen atoms of two DPC^{2-} ions resulted with a distorted octahedral conformation. The complex **4** consists of two independent and different cationic Cu(II) sites. Cu(II) atoms are coordinated by two N atoms, one from DPC^{2-} and one from SMABT ring, two carboxylate O atoms from DPC and one water molecule to give distorted square pyramidal structures. Intermolecular N-H…O and O-H…O hydrogen bonds and π-π stacking interactions seem to be effective in the stabilization of the crystal structure. Elemental analyses and all measurements show good agreement with the structures.

The newly synthesized compounds (**1**-**4**) in the present study possess significant inhibition effect on hCA I and on hCA II for hydratase and esterase activities. The inhibitory effects of the compounds on CA isoenzymes are comparable to those of the AAZ compound, and they should be subject to further inhibition *in vivo* tests.

5. Supplementary data

CCDC 1559299 (**2**), CCDC 1559300 (**3**), and CCDC 1559301 (**4**) contain supplementary crystallographic data for this paper. This data can be obtained free of charge via http://www.ccdc.cam.ac.uk (the Cambridge Crystallographic Data Centre, 12 Union Road, Cambridge CB2 1EZ, UK; fax (+44 1123 336 033; or email: deposit@ccdc.cam.ac.uk).

Acknowledgments

The authors acknowledge the support provided by Dumlupınar University Research Fund (grant No. 2014/18). In addition, the authors acknowledge Aksaray University of Science and Technology Application and Research Center, for the use of the Bruker SMART BREEZE CCD diffractometer (purchased under grant No. 2010K120480 of the State of Planning Organization).

References

[1] G. Achaiah, N.S. Goud, K.P. Kumar, P. Mayuri, Int. J. Pharm. Sci. Res. 7(4) (2016) 1375-1382.

[2] P.S. Yadav, G.P. Senthilkumar, Int. J. Pharm. Sci. Drug Res. 3(1) (2011) 01-07.

[3] R.K. Gill, R.K. Rawal, J. Bariwal, Arch. Pharm. Chem. Life Sci. 348 (2015) 155–178

[4] H. Aghabozorg, F. Manteghi, S. Sheshmani, J. Iran. Chem. Soc. 5(2) (2008) 184-227.

[5] D.L. Hoof, D.G. Tisley, R.A. Walton, J Chem. Soc. Dalton Trans., 2 (1973) 200-204.

[6] L. Yang, D.C. Crans, S.M. Miller, A. La Cour, O.P. Anderson, P.M. Kaszynski, M.E. Godzala, III, L.D. Austin, G.R. Willsky, Inorg. Chem., 41 (2002) 4859-4871.

[7] P. Buglyo´, D.C. Crans, E.M. Nagy, R.L. Lindo, L. Yang, J.J. Smee, W. Jin, L.H. Chi, M.E. Godzala, III, G.R. Willsky, Inorg. Chem., 44 (2005) 5416-5427.

[8] C. Yenikaya, N. Büyükkıdan, M. Sarı, R. Keşli, H. İlkimen, M. Bülbül, O. Büyükgüngör, J. Coor. Chem. 64(19) (2011) 3353-3365.

[9] C. Yenikaya, M. Poyraz, M. Sarı, F. Demirci, H. İlkimen, O. Büyükgüngör, Polyhedron 28(16) (2009) 3526-3532.

[10] H. İlkimen, C. Yenikaya, M. Sarı, M. Bülbül, E. Tunca, Y. Süzen, Polyhedron 61 (2013) 56-64.

[11] H. İlkimen, C. Yenikaya, M. Sarı, M. Bülbül, E. Tunca, H. Dal, J. Enzyme Inhib. Med. Chem. 29(3) (2014) 353-361.

[12] H. İlkimen, C. Yenikaya, M. Sarı, M. Bülbül, E. Tunca, H. Dal, J. Enzyme Inhib. Med. Chem. 30(2) (2015) 195-203.

[13] H. İlkimen, C. Yenikaya, A. Gülbandılar, M. Sarı, J. Mol. Struct. 1120 (2016) 25-33

[14] N. Büyükkıdan, C. Yenikaya, H. İlkimen, C. Karahan, C. Darcan, E. Şahin, Russian J. Coor. Chem. 39(1) (2013) 96-103.

[15] H.P. Kaufmann, J.H. Buckmann, Arch. Pharm. 279(6) (1941) 194-209.

[16] Z.A. Alkaya, H. İlkimen, C. Yenikaya, Y. Kaygısız, M. Bülbül, T. Tunç, M. Sarı, J. Enzyme Inhib. Med. Chem. 32(1) (2017) 231-239.

[17] G. Anderegg, E. Bottari, Helvetica Chimica Acta 48(4) (1965) 887–892.

[18] L.E. Riafrecha, S. Bua, C.T. Supuran, P.A. Colinas, Bioorg. Chem. 76 (2018) 61-66.

[19] F. Erdemir, D.B. Celepci, A. Aktaş, P. Taslimi, Y. Gök, H. Karabıyık, İ. Gülçin, J. Mol. Struct. 1155 (2018) 797-806.

[20] D. Ekinci, H. Çavdar, O. Talaz, M. Şentürk, C.T. Supuran, Bioorg. Med. Chem. 18 (2010) 3559-3563.

[21] S. Schwarz, S. Sommerwerk, D.S. Lucas, L. Heller, R. Csuk, European J. Med. Chem. 86 (2014) 95-102.

[22] S. Angapelly, P.V. Sri Ramya, A. Angeli, S. Del Prete, C. Capasso, M. Arifuddin, C.T. Supuran, Bioorg. Med. Chem. 25(20) (2017) 5726-5732.

[23] E.E Rickli, S.A.S Ghazanfar, B.H. Gibbons, J.T. Edsall, J. Biol. Chem. 239 (1964) 1065-1078.

[24] M.M. Bradford, Anal. Biochem. 72 (1976) 248-254.

[25] U.K. Laemmli, Nature 227 (1970) 680-685.

[26] K.M. Wilbur, N.G. Anderson, J. Biol. Chem. 176 (1948) 147-154.

[27] J.A. Verpoorte, S. Mehta, J.T. Edsall, J. Biol. Chem. 242 (1967) 4221-4229.

[28] C. Yenikaya, H. İlkimen, M.M. Demirel, B. Ceyhan, M. Bülbül, E. Tunca, J. Brazilian Chem.Soc. 27(10) (2016) 1706-1714.

[29] H. Lineweaver, D. Burk, J. American Chem. Soc. 56(3) (1934) 658-666.

[30] Bruker, SADABS, Bruker AXS Inc. Madison; 2005.

[31] G.M. Sheldrick, SHELXS97 AND SHEXL97. Program for Crystal Structure Solution and Refinement. University of Gottingen, Germany, 1997.

[32] L.J. Farrugia, J. Appl. Cryst. 30 (1997) 565-565.

[33] A.W. Addison, T.N. Rao, Chem. Soc. J Dalton Trans. 1 (1984) 1349-1355.

[34] Y.F. Sun, J.R. Lu, Z.B. Zheng, Acta Cryst. E63 (2007) m1881-m1881.

[35] J. Hermle, G. Meyer, Acta Cryst. E67 (2011) m1089-m1089.

[36] M. Shahid, M. Mazhar, M. Helliwell, J. Akhtar, K Ahmad, Acta Cryst. E64 (2008) m1139-m1140.

[37] D. Cook, Canadian J. Chem. 39(10) (1961) 2009.

[38] K. Nakamoto, Infrared and Raman spectra of inorganic and coordination compounds, 5th Edition, Interscience-Wiley, NewYork, 1997 p 232.

[39] W.J. Geary, Coord. Chem. Rev. 7 (1971) 81-121.

Tables and Figures

Table 1. Crystal data and structure refinement details for compounds **2-4.**

Table 2. Selected bond distances [Å] and angles [°] of compounds **2-4.**

Table 3. Hydrogen bonds for compounds **3** and **4** (Å, °)

Figure 1. Syntheses of all compounds (**a** for **2** and **b** for **3** and **c** for **4**).

Figure 2. The molecular structure of (**2**), with atom labels and 50% probability displacement ellipsoids for non-H atoms [Symmetry code: (i) $-x + 1, -y + 1, -z + 1$].

Figure 3. The molecular structure of (**3**), with atom labels and 50% probability displacement ellipsoids for non-H atoms.

Figure 4. The molecular structure of (**4**), with atom labels and 50% probability displacement ellipsoids for non-H atoms.

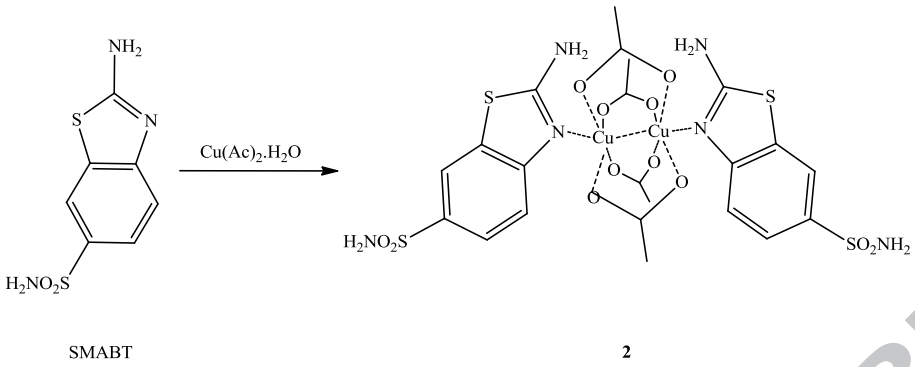

SMABT **2**

(**a**)

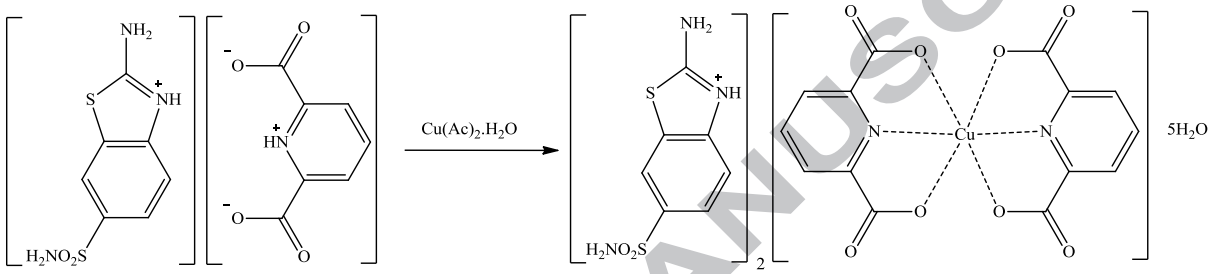

1 **3**

(**b**)

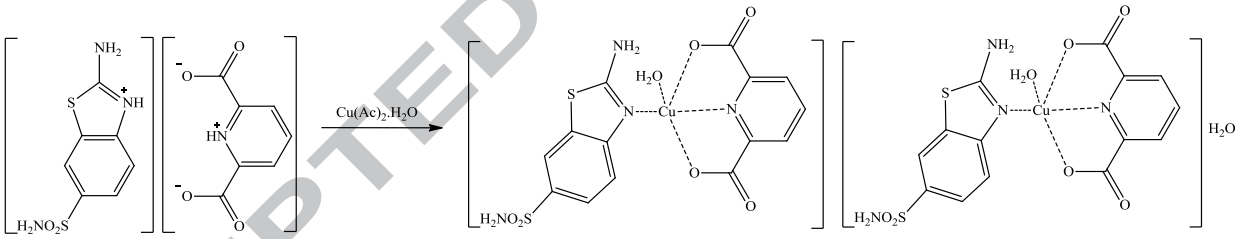

1 **4**

(**c**)

Figure 1. Syntheses of all compounds (**a** for **2** and **b** for **3** and **c** for **4**)

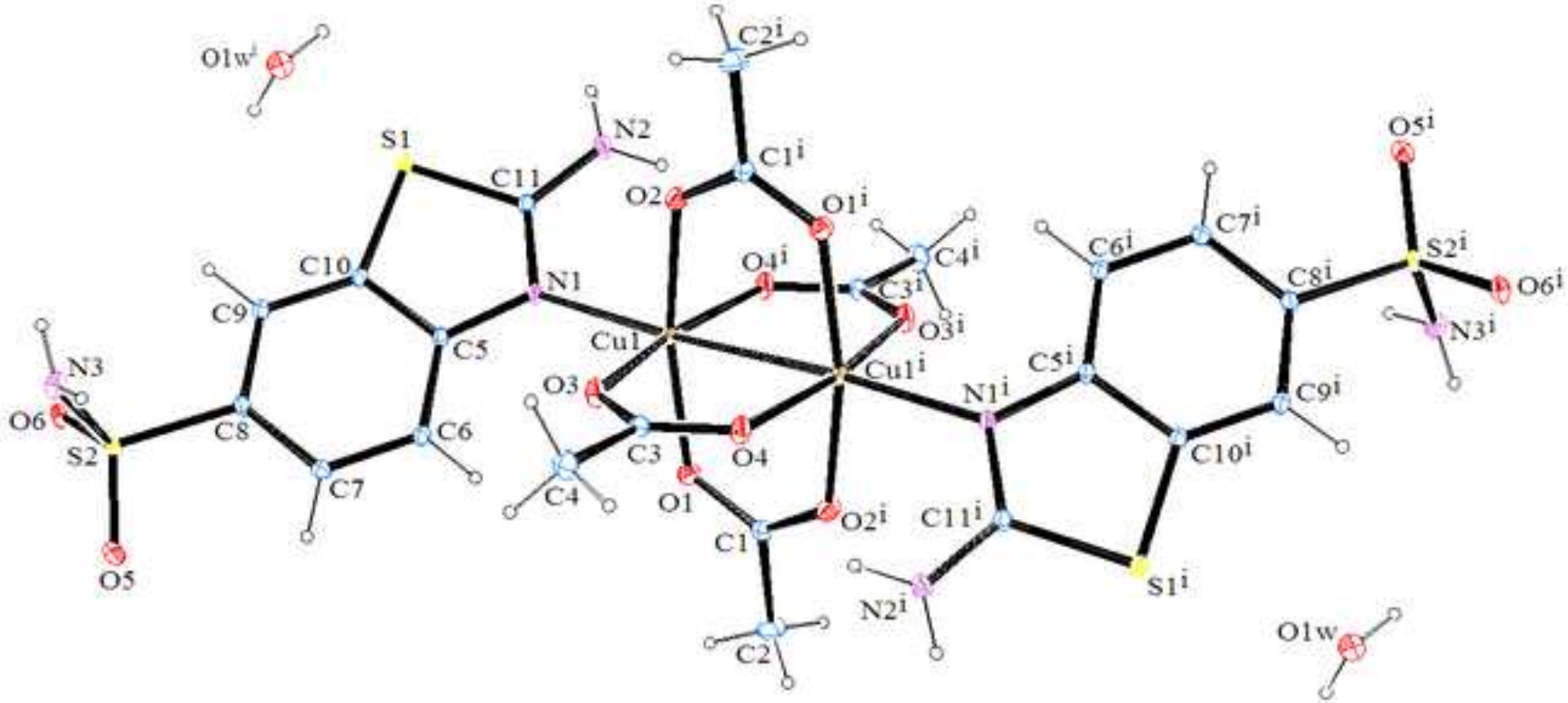

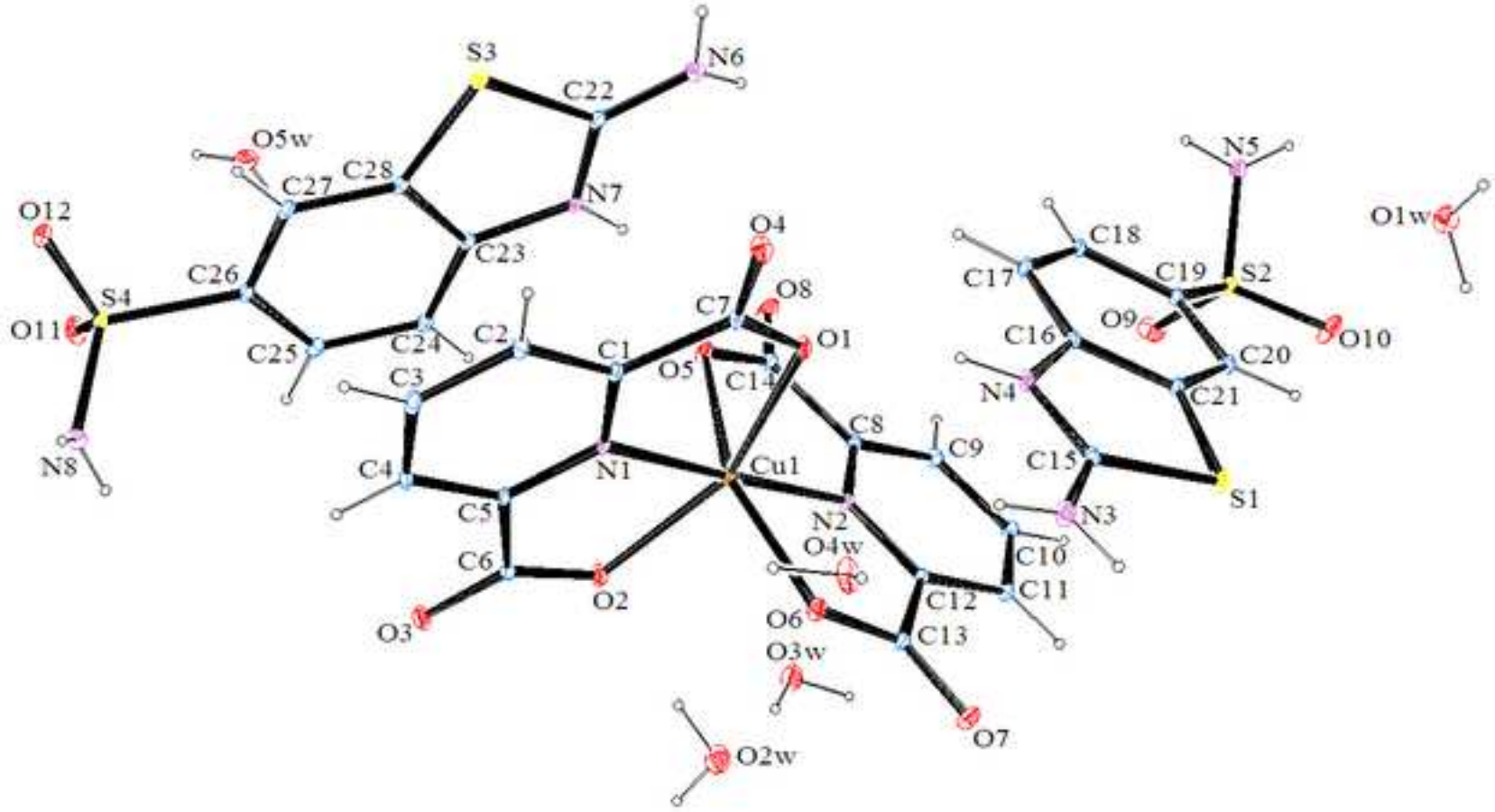

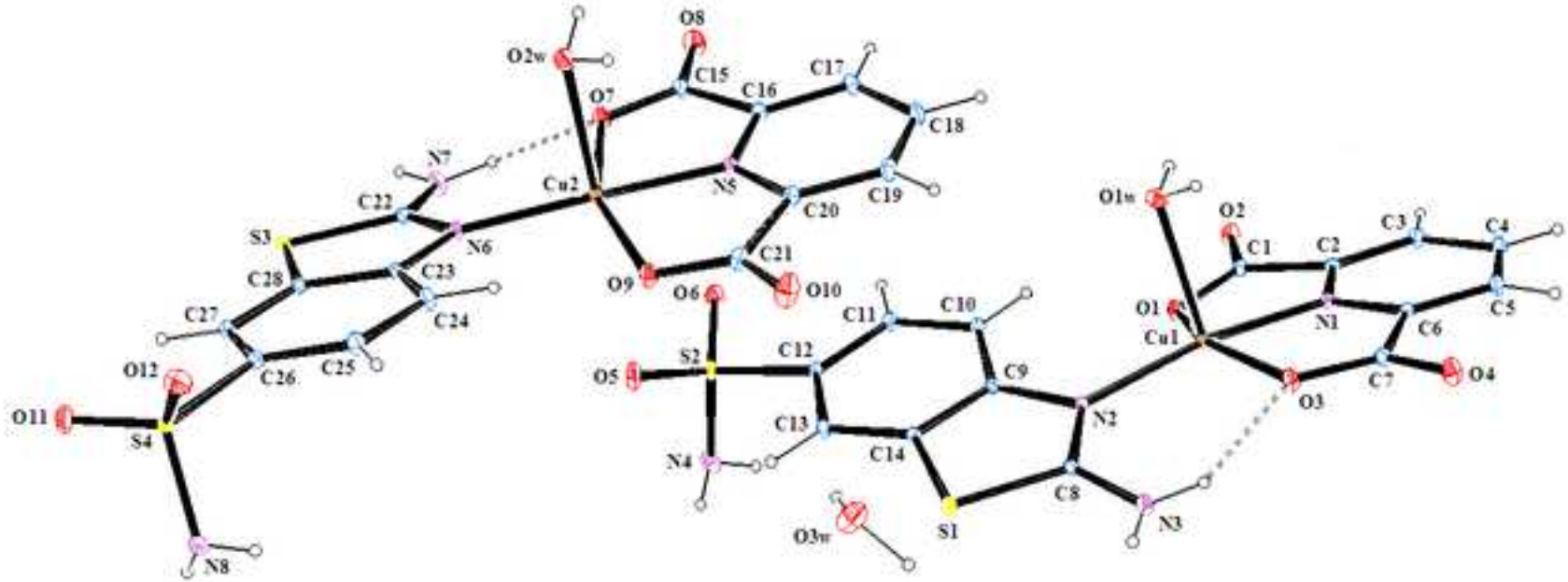

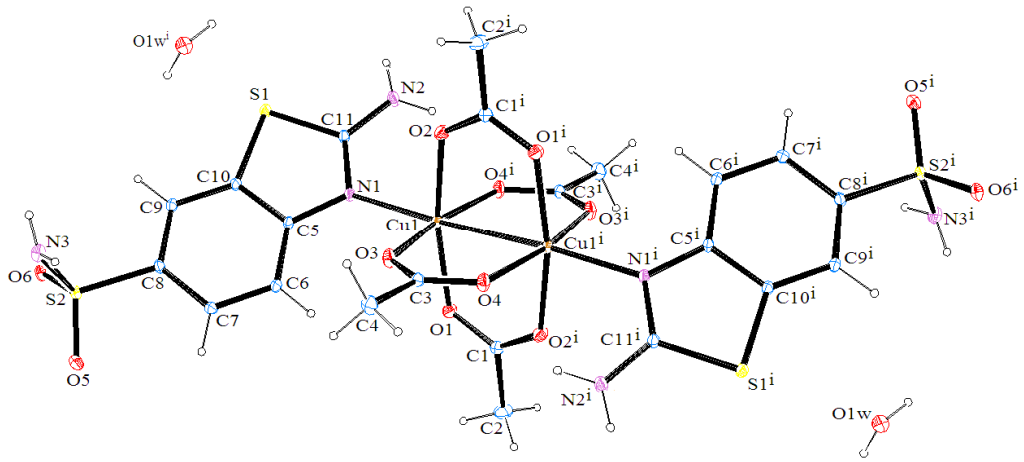

Newly synthesized Cu(II) complexes of 2-amino-6-sulfamoylbenzothiazole (**2-4**) have effective inhibitory activity on hCA I and II. **2** and **3** crystallize in the triclinic $P\bar{1}$ space group with distorted octahedral conformations. **4** crystallizes in the monoclinic P2/1c space group and has distorted square pyramidal structure.